General properties of the spectrum of complex scaled Hamiltonians: Phenomenological description of pole string curves

H. Lehr and C. A. Chatzidimitriou-Dreismann
I. N. Stranski-Institute for Physical and Theoretical Chemistry, Technical University of Berlin, Strasse d. 17. Juni 112, D-10623 Berlin, Federal Republic of Germany

(Received 26 October 1993; revised manuscript received 22 February 1994)

This study is devoted to the general properties of pole strings and string curves of the eigenvalues of complex scaled Hamiltonians; in detail, it is our aim to correlate parameters of the Hamiltonian (mass and parameters of the potential) to the shape and location of the corresponding string curve. In the present contribution, which considers one-dimensional Hamiltonians, we show that every string curve can be decomposed into a few, very simple "primitives." The latter are associated with certain subunits (or parts) of the potential in such a way that each subunit gives one and only one string curve. If a potential under investigation contains more than one subunit, then one will find multiple or composite string curves. The corresponding Hamiltonian will posses an additional symmetry that can be expressed by introducing a combined index (n,m), where n numbers the subunit and m the resonant eigenvalue belonging to the subunit. Furthermore we show in this contribution phenomenologically which kind of string curve emerges from which type of subunit; one is able to predict the general shape of the string curve and some of its inherent information. The mass dependence (or nondependence) of the string curves is explicitly discussed and parallels with the semiclassical WKB theory are addressed. In addition we present material concerning the possible "wiggly" behavior of pole strings; we show explicitly on the the semiclassical level why certain potential features wiggle while others do not. Employing semiclassical concepts, we are even able to "explain" the corresponding string curves in terms of simple integrals. We also give a condition—depending only on the zeros of the function $E - V(z)$—for the possible emergence of wiggles. Numerical experiments that are partly reported here show that all potentials with a Gaussian damping factor posses wiggles, while those with exponential damping (e^{-x}) do not.

PACS number(s): 34.10.+x, 03.65.Nk, 11.55.Fv, 11.55.Bq

I. INTRODUCTION

In the years since the discovery of complex scaling [1–4] many articles on very different aspects of the complex scaling method and its applications have appeared (see, e.g., [5–8], and references therein). Missing, however, is a more general description of resonance strings. Though resonances are naturally not connected with complex scaling exclusively, the latter being a theory that we find to be very clean and almost "natural," we will use this theory always as our reference point in the sense that here we will regard results of complex scaling as "true," i.e., we have not taken upon us to check whether other approaches like complex angular momentum or a rigged Hilbert space theory, to name only two other possibilities (see, e.g., [5,9–11], and references therein), will give the same results. For the present contribution therefore we will only talk of the spectra of complex scaled Hamiltonians, disregarding the fact that the same results might well have been produced by other theoretic approaches.

So what we do want to do is to go a step in the direction of describing somewhat more general resonance strings and to try to understand how they come about. In the present paper we will focus on one-dimensional problems, since—as we know from our experience—higher dimensional problems are substantially more complicated. More specifically, we present material mostly from the following classes of potentials: (1) $P(x)$ with uneven order or negative leading coefficient, (2) $P(x)e^{-cx}$, and (3) $P(x)e^{-cx^2}$, where $P(x)$ is a polynomial.

Since the work of Rittby, Elander, and Brändas [12–14] it is a known fact that the eigenvalues of the complex scaled Hamiltonian (see Appendix B for a short summary of our nomenclature) are not scattered "at random" in the complex plane. Rather they occur in a very ordered manner, in so-called *strings*; cf. Fig. 1. Let us clarify briefly the terminology that will be used throughout this article. We will call a string the set of eigenvalues belonging to the discrete part of the spectrum of a specific Hamiltonian and a pole trajectory will denote the "path" that a specific eigenvalue undertakes, when changing parameters like mass or potential height, etc. We will use the words "resonance" and "pole" synonymously (for some numerical details, see Appendix B). Furthermore, we will use the term *string curve* as the (parametric) function that comes about by connecting the resonant poles in the complex plane. Korsch introduced the term string curve [15] and defined it in a WKB manner as

$$\mathfrak{N} = \frac{1}{\pi}\int q(z)\,dz - \tfrac{1}{2} \in \mathbb{R}, \tag{1}$$

with the function $q(z)$ in its simplest form being (we are using atomic units throughout, so $\hbar = 1$)

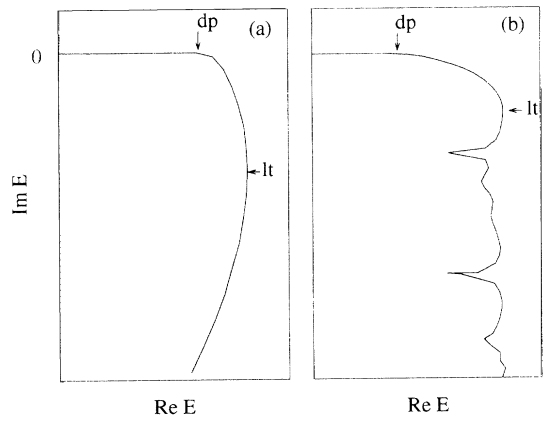

FIG. 1. Two of the most common string curves. (a) shows a smooth string curve, while (b) shows a wiggly string curve. Indicated in the figure are the detachment point ("dp") and the localization threshold ("lt"). See text for further details.

$$q(z) = \sqrt{2\mu[E - V(z)]}$$

where E is complex [for physical reasons $\mathrm{Im}(E) \leq 0$] and $V(z)$ is the analytical continuation of the potential into the complex plane (μ is the mass of the system). Higher order results can be found using the phase integral method [16,17] or higher order WKB approximations.

The integral in Eq. (1) extends from one so-called transition point, i.e., a point of the complex plane where $q^2(z)$ vanishes, to another. The definition (1) is correct if and only if one pair of transition points is relevant, (see below); it uniquely defines a curve in the complex energy plane. If $\mathfrak{N}$ is not only real, but also integer, it is identical with the quantum number describing the eigenstates. At those points Eq. (1) reduces to the generalized Bohr-Sommerfeld formula for (complex energy) resonances (see, e.g., [15,16]).

Note that the applicability of Eq. (1) is somewhat limited, because one may well have to include more than one pair of transition points. The generalized definition reads for a symmetric potential

$$\mathfrak{N} = -i \ln \left(\sum_{r=1}^{n} e^{2i\alpha_{0r}} \right) \in \mathbb{R}, \tag{2}$$

with

$$\alpha_{0r} = \int_0^{t_r} q(z)\, dz, \tag{3}$$

where n is the number of relevant transition points t_r. Equation (2) simply follows from the outgoing wave boundary condition embedded into the WKB formalism [15,16], if $\mathfrak{N}$ is a half-integer multiple of π.

Though the definition in non-WKB terms is somewhat less obvious, we found that the concept of a string curve is a very promising and intuitive one for handling more general descriptions of the spectra of Hamiltonians; see below.

Our goal is an as complete as possible characterization of a string curve via "physical" terms, i.e., the potential parameters and possibly the mass of the system; see below. Naturally, this question could never be answered in terms of individual poles, because that would mean finding a way around solving the Schrödinger equation. Besides being interesting on its own, a study of pole string curves seems important to us, because of several reasons.

Almost all studies employing complex scaling use model Hamiltonians to calculate eigenenergies and/or states for physical problems. There are very few examples of Hartree-Fock (HF) or even configuration-interaction (CI) calculations (see, e.g., [18–20], and references therein). The usual problem with model Hamiltonians is the question of the choice of parameters to fit the experimental situation. By choosing a specific representation (i.e., analytical form) and a set of parameters one always introduces a certain amount of arbitrariness into the calculation. Therefore one should ideally be able to distinguish between a physical result and a result introduced into the system by the choice of form and parameters. Thus it is necessary to know how a change in the parameters will affect the results, and to know what special effects one can expect by choosing a specific representation.

Secondly, there exist claims that pole strings are connected with the microcanonical (unimolecular) reaction rate, when the dominant reaction mechanism is tunneling (for shape resonances that we consider here only); see, e.g., [21]. The usual interpretation of the half of the negative imaginary part of the energy as inverse lifetime (divided by $\hbar$; this interpretation goes back at least to Gamow [22]) gives us a chance to evaluate this rate without receding to quasiclassical concepts like the usual "frequency times transmission coefficient" (see, e.g., [23]). That the interpretation as lifetime and therefore as rate constant is essentially correct has been claimed by Moiseyev *et al.* [21] and also by Seideman and Miller, who have published recently on the intimate connection of complex poles and the microcanonical rate [24]. Naturally, the rate is a continuous function of the (real) energy, while the set of eigenvalues is discontinuous. We believe that the string curve corresponds to the continuous rate vs energy curve; work along these lines is in progress [25]. For studying the tunnel effect one might draw the conclusion that it appears more natural to study string curves instead of poles.

II. INFLUENCE OF THE MASS ON STRING CURVES

What makes the study of pole string curves especially rewarding is the fact that the part of the string curve having a clearer physical interpretation (the one we will call later on *regular*; see below) *does not—in first order—depend on the mass* for (real) energies above the potential height. Naturally the position of the eigenvalues in the complex plane does depend on the mass, but in such a way that they stay on the string curve. For energies below the potential height (the detachment point, see below) and above the localization threshold (see below and Fig. 1), however, the string curve is not indepen-

dent of the mass. In Fig. 2 we show the spectrum of $V(x) = (ax^2 - b)e^{-x^2}(a = 35, b = 5.6)$, a potential whose analytical form (though not the parameters) has been used frequently in the literature [12–15,26], for different masses. Please note that due to the plot scale the first parts of the strings (up to the detachment point) seem to be identical. For a more quantitative check we calculated the imaginary energy for different masses, which were chosen in such a way that the real parts of the energies are—with three to four digits—the same. As can be seen from Table I the imaginary energies for a resonance below the detachment point differ by about three orders of magnitude when changing the mass by about two orders of magnitude. The same procedure applied to a resonance above the detachment point gives a change by about 4%, which is considerably less.

This rather surprising result is consistent with the WKB analysis of the problem (especially with that of Andersson [27]). For energies below the potential height (= barrier maximum)—but above the threshold [$= \lim_{|x|\to\infty} V(x)$, by convention set to zero]—it is necessary to include all four transition points, if one thinks of a double barrier potential for the moment, in order to get a nonvanishing imaginary part of the energy; see, e.g., [15,16]. (Because of symmetry, though, the calculations can be reduced to using two of them.) For energies above the potential height, Andersson has shown in his paper [27] that only two (one if symmetry is considered) transition points need to be considered. That is, to find the approximate resonance energies one considers the (generalized) Bohr-Sommerfeld formula Eq. (1) (naturally, $\mathfrak{N}$ is here required to be integer) with zero as lower and t_1, which lies in the first quadrant of the complex coordinate plane, as upper limit.

If one now considers string curves instead of individual poles it is obvious from the definition Eq. (1), namely, that $\mathfrak{N}$ must be real, that the mass—being real—does not play any role. That is, whenever only one transition point must be considered the string curve as defined by Eq. (1) is not mass dependent. Or, to reverse the last sentence (which is preferable because of the approximative nature of the WKB ansatz), whenever the string curve is mass dependent one must consider more than one transition point. Otherwise the predicted (non-)mass-dependence is incorrect.

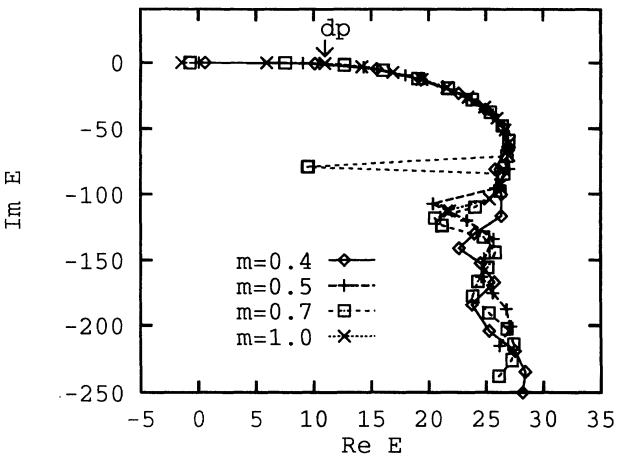

FIG. 2. Pole string curves of $V(x) = (35x^2 - 5.6)e^{-x^2}$ for different masses (m in the plot) in the range of 0.4 to 1.0. Depicted is the regular and (wiggly) irregular part. Below the detachment point ("dp" in the figure) and above the localization threshold the string curve depends on the mass, while it is to first order independent of the mass elsewhere. See also Table I for numerical details.

III. NOMENCLATURE FOR POLE STRINGS

Let us start the phenomenological description of string curves by introducing a nomenclature for them, which will be explained in the next section.

If one has in mind a potential that consists of at least one well plus a "minimal" environment, i.e., two barriers (one of which may be nontransparent, i.e., of infinite height) the typical string curve looks like either Fig. 1(a) or Fig. 1(b). For certain reasons that will be described below we divide these string curves in two parts, namely, the one up to the *localization threshold* (lt in Fig. 1), which in this case coincides with a threshold in real energy, and the one after that. We will refer to these parts as *primitives* of which a string curve consists. The primitive below the localization threshold ("below" always referring to the smaller quantum number) will be called *regular*, while the other will be called the *irregular* part

TABLE I. Comparison of the mass dependence of complex eigenvalues below and above the detachment point for the potential $V(x) = (0.5x^2 - 0.8)e^{-0.1x^2}$ The mass was chosen such that the real part is constant to three to four digits. Below the detachment point ("dp" in the table) the imaginary part changes by about three orders of magnitude when the mass changes by two orders, while for energies above the detachment point the imaginary part is almost independent of the mass. In the table $(-n)$ means 10^{-n}; units are atomic.

Below dp			Above dp		
Mass	Re E	Im E	Mass	Re E	Im E
0.3330	2.1265	5.8999(-2)	0.2724	4.0554	3.40819
1.0000	2.1272	1.5447(-2)	1.0000	4.0554	3.29864
5.0600	2.1273	7.4147(-4)	3.3500	4.0556	3.27009
9.5050	2.1243	1.1214(-4)	6.4550	4.0557	3.26444
12.2500	2.1228	4.4281(-5)	10.6560	4.0559	3.26276
15.2500	2.1261	2.0630(-5)	14.7700	4.0553	3.25931

of the string curve. An irregular part can be of *smooth* type, as in Fig. 1(a), or of *wiggly* type, as in Fig. 1(b). One of those "peaks" in Fig. 1(b) will be called here a *spike*. Another important feature of string curves is that they "detach" at a certain real energy from the real axis, i.e., below the *detachment point* (dp in the figure) the string curve stays very close to the real axis, while after it moves rapidly into the complex plane; see below.

More generally speaking, the spectrum of a Hamiltonian can contain no, one, or multiple string curves. One of the string curves can consist of an irregular part, a regular and an irregular part, or one regular and two irregular parts (see, e.g., Fig. 6 below). The first two types will be called *simple*, while the third one will be called *composite*.

IV. A MORE DETAILED DESCRIPTION OF STRING CURVES

Let us for the moment think of a simple double barrier or a one-barrier–one-wall ("wall" means a barrier of infinite height) combination. The potential might have one or more bound states. The corresponding wave functions are naturally localized in the potential well having one or more nodes. If we move up with the energy above the threshold [i.e., the $\lim_{|x|\to\infty} V(x)$; usually set to zero] tunneling is possible and the static description using the real axis fails. By using complex scaling [2,3,28] we "filter out" certain quasibound states that one calls resonances, since if the imaginary part of the corresponding energy is small, they coincide with sharp peaks in the scattering cross section or in the transmission coefficient [29]. As mentioned, these quasibound states belong to complex energy eigenvalues of the complex rotated Schrödinger equation. The imaginary part of the energy rises with the quantum number (in a single string curve). Up to the detachment point, however, it stays rather small, while after it it rises rapidly. We found that this detachment point coincides with the height V_0 of the potential above the threshold. This is seen best if one calculates the "density of states" $\rho(E)$,

$$\rho(E) \equiv \frac{dn}{d|E|} \approx \frac{2}{|E_{i+1} - E_{i-1}|} \tag{4}$$

(note that we chose the modulus in order to measure the "real" distance between the poles). As one can see from Fig. 3, the density has a sharp peak at $V_0 = 2.36$ hartree, so we can speak of a detachment *point*. The solid lines in Fig. 3 are the result of a WKB calculation. There we evaluated the density of states via

$$\frac{d\Re}{dE} = \frac{2\mu}{\pi} \int_0^{t_1} \frac{1}{q(z)} dz. \tag{5}$$

Note that we have used *real* energies for this calculation. One sees that the excellent agreement before the potential height of 2.36 hartree is somewhat diminished after it. Nevertheless, the "predicted" WKB density clearly has the correct shape.

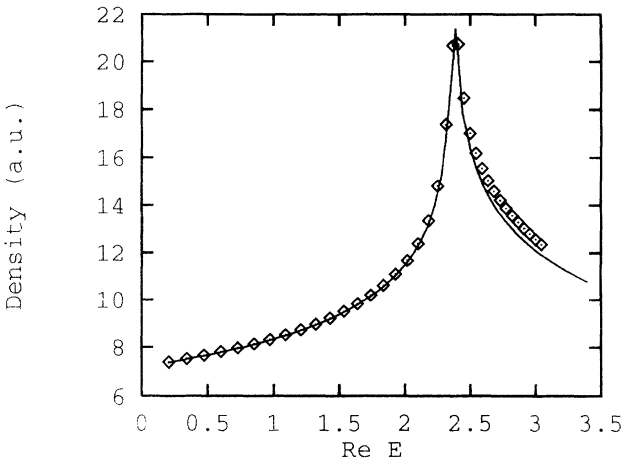

FIG. 3. Density of eigenvalues for $V(x) = (0.5x^2 - 0.8)e^{-0.1x^2} + 0.8$ and $\mu = 60$ a.u. with a peak around the potential height of 2.36 hartree. This indicates that there is indeed a detachment *point* and not a smooth transition. The solid line is the result of a WKB calculation evaluating Eq. (5) using *real* energies. The agreement is good throughout, although it necessarily diminishes for higher energies.

If one raises the real energy more and more, the lifetime of the resonances (proportional to the inverse of the imaginary part of the energy) shortens ever more. This is true until we reach a certain point, namely, the *localization threshold*. From this point on the lifetime either shortens with dropping real energy (smooth type) or has a more complicated dependence on the real energy (wiggly type); cf. Fig. 1. The localization threshold coincides very often with a bound in the real energy, however, it does not necessarily: e.g., for the potential $V(x) = (ax^4 + b)e^{-cx^2} (a = 87, b = -5.6, c = 2)$, there seems to be no threshold in real energy. Generally speaking, this coincidence depends on the choice of parameters of the potential. The localization threshold was called the *complex threshold* by Rittby, Elander, and Brändas [13] to indicate the "borderline" between primary poles (regular part) and secondary poles (irregular part). However, we feel that the nomenclature of the present authors is more to the point for the following reason. We believe the physical mechanism constituting the complex energy eigenvalues to change at the localization threshold. One should expect of a quasibound state that it is localized *between* the barriers. This is true for all resonances up to the localization threshold. At this point, however, the localization pattern changes within a few quantum numbers from localization within the attractive region of the potential (say, for a symmetric double barrier potential $-x_{\max} < x < x_{\max}$, where $x_{\max}$ is the position of the potential maximum) to localization beneath that region, i.e., just outside the attractive region of the potential. Figure 4 shows this behavior for the well-known potential $V(x) = (0.5x^2 - 0.8)e^{-0.1x^2} + 0.8$, which has been used extensively in the literature [13–15,26]. It should be noted that in this figure we plotted $|\psi_n(\theta = 0.75)|^2$ and we normalized ψ_n according to the "standard" $\mathcal{L}^2$ way, i.e.,

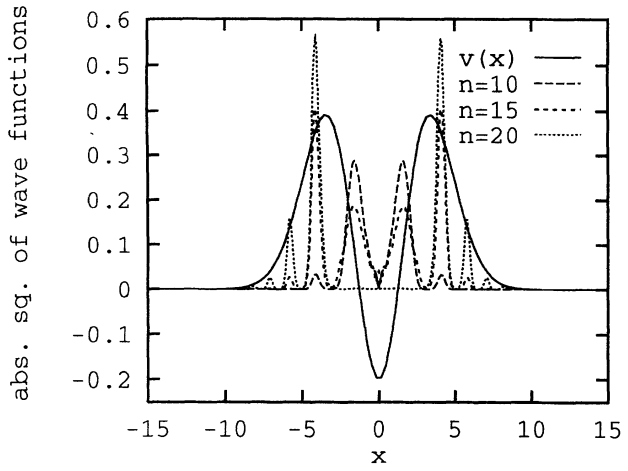

FIG. 4. The absolute square $|\psi|^2$ of selected wave functions of $V(x) = (0.5x^2 - 0.8)e^{-0.1x^2} + 0.8$ ($\mu = 1$) plus the potential itself (scaled by a factor of 1/6). The quantum number $n = 10$ is equivalent to an energy below the localization threshold, $n = 15$ is at the localization threshold, and $n = 20$ corresponds to an energy above the localization threshold. As can be seen in the figure, the localization pattern changes drastically from being localized within the well to being localized beneath the barriers. Please note that the localization pattern is quite independent of the angle θ. For graphical reasons the wave functions are normalized in the standard $\mathcal{L}^2$ way instead of using the (correct) complex scaling method (CSM) way [Eq. (B5)].

$$\int_{-\infty}^{+\infty} [\psi(\eta x)]^* \psi(\eta x)\, \eta\, dx \;=\; 1.$$

This is not the correct way to normalize, if one uses complex scaling, where it can be shown that one has to use a different scalar product (see Appendix B); nevertheless, the localization pattern does not depend significantly on either the angle θ (as long as it is large enough, naturally) or the normalization procedure used. (Using the correct scalar product has the "disadvantage" that the resulting moduli of the wave functions differ by orders of magnitude, so comparison is very complicated. In order to facilitate comparison—and since the resulting localization pattern is not affected—we decided to use the incorrect scalar product.) We therefore conclude that this is a meaningful procedure for our purpose at this point.

We assume that the physical mechanism leading to the resonances is changing in the respect that, below the localization threshold, we have tunneling. Particles are trapped "between" the barriers (note that the real part of the energy is far above the potential maximum) for a certain—near the localization threshold rather short—time. But every finite potential (i.e. a potential that has no attractive poles) has a limited "localization ability," i.e., it cannot hinder significantly any particles with an energy higher than a certain value. This value we believe to be the localization threshold. We assert that the states with higher quantum number correspond to a (retarded) backscattering. Our assertion is supported by the fact that a single barrier (like a Gaussian barrier, e.g.) has no regular part at all, but only an irregular part; see Fig. 5. Using our argumentation this behavior is obvious: Since there can be no quasibound situation, because of the missing well, there can be no regular part. On the other hand, there might be both "free" states and states that are scattered back that correspond to the eigenvalues above the localization threshold. Looking at the localization only is here clearly not sufficient. A detailed dynamical study should shed some light onto the matter.

Generalizing the discussion now, let us briefly outline what string curves one has to expect for what kind of potentials. In the simplest case we have a single barrier only. For such potentials we always find an irregular part starting at the height of the barrier, i.e., localization threshold and detachment point coalesce. For Gaussian barriers we found smooth irregular parts up to high imaginary energies. Closer inspection revealed, though, that they do have a wiggly irregular part starting only relatively deep in the complex energy plane (see Fig. 5). As mentioned above there can be no regular string curve. We found irregular parts starting at the height of the barrier also, if one has within a potential a very pronounced single barrier; see below.

The next case would be a one-well–one-barrier combination. Here we have both a pronounced single barrier and some trapping because of the well. Therefore we find a *composite* string curve consisting of both a regular string curve detaching at zero (the lowest barrier "available") and an irregular string curve starting at the potential height above zero. The two string curves coalesce. This "bifurcation" point depends on, e.g., the attractivity of the potential, i.e., the depth of the potential minimum. This effect is shown in Fig. 6, where we depict a number of resonance string curves for potentials of the family $V(x) = a(x + b)e^{-x^2}$ (see Appendix A for

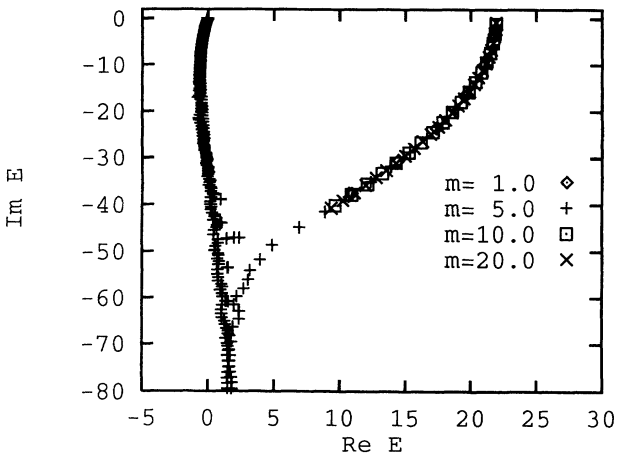

FIG. 5. Spectrum of a simple Gaussian barrier $V(x) = 21.944e^{-x^2}$ for four different masses ($\mu = 1, 5, 10, 20$; m in the figure). There is an irregular part only and this part (up to a certain imaginary energy) does not depend on the mass. For $\mu = 5$ the "complete" spectrum is shown, i.e., resonances plus eigenvalues of the kinetic energy operator. Please note that the string is wiggly.

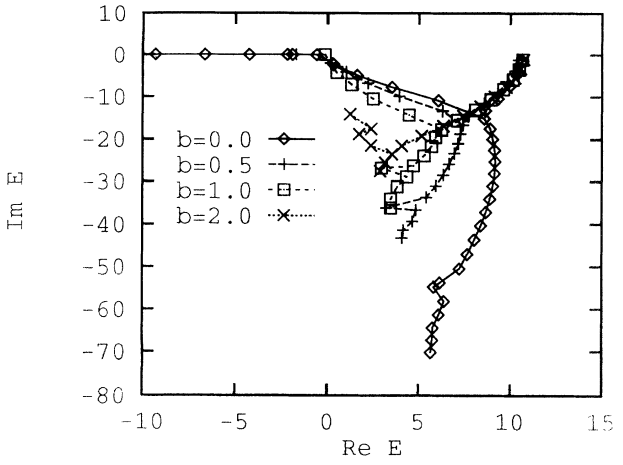

FIG. 6. Composite pole string curves for $V(x) = a(x+b)e^{-x^2}$ for different choices of the parameter b, which affects the asymmetry, i.e., the depth of the well. The "bifurcation point" moves into the complex plane when lowering the depth of the well (raising b). It can also be seen that the first irregular part starting at the potential height is relatively independent of the choice of b. The lines connecting the poles are just a guide for the eye. See also Table IX below.

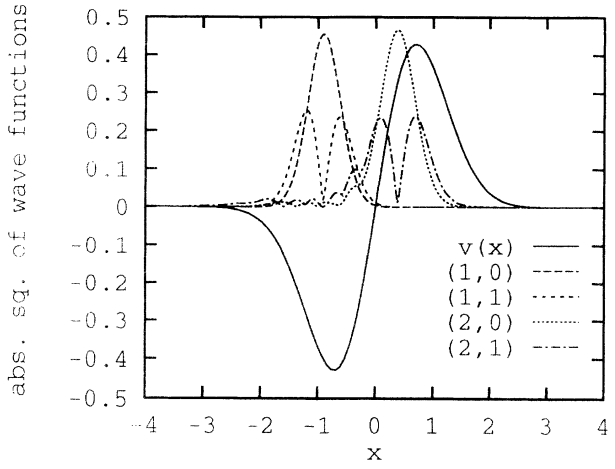

FIG. 7. The absolute square $|\psi|^2$ of some selected wave functions of $V(x) = 25xe^{-x^2}$ with $\mu = 5$. Depicted are the potential (scaled by 1/25), the first bound states, and the first wave functions that belong to energies that constitute the first irregular part of the string curve; see Fig. 6. Apparently the latter wave functions can also be classified by a quantum number (starting at zero) and the complete description of the string curve involves two quantum numbers (consequently, we have numbered the wave functions in that manner in the figure). This in turn indicates that we have two irreducible units in this potential, namely, the barrier itself and the barrier-well combination.

the detailed choice of parameters). We changed there the potential depth, while keeping the height of the barrier constant. As one can see, the "bifurcation point" moves upwards as we increase the "attractivity" of the potential. From a certain depth on, though, we find a kind of saturation, i.e., the "bifurcation point" does not alter any more.

By inspection of the corresponding wave functions of the (point-) symmetric one of this potential family ($a = 25, b = 0.0$) we can observe something rather surprising (see Fig. 7): Apparently the "backscattering" resonances of the irregular part starting at V_0 have zero, one, two, etc. nodes, so we might label them by a quantum number starting at zero. Since the same is true for the bound states and the first resonances, we may already here be tempted to argue that two quantum numbers are necessary: one labeling the string curve and one labeling the number of the eigensolution within the string curves. As we will argue below, this potential consists of two irreducible units (namely, the barrier only and the barrier plus well), therefore needing two quantum numbers to label an eigensolution uniquely.

For a symmetric double barrier we should expect to find a simple string curve, which indeed is true. The string curve may be either smooth or wiggly. For nonsymmetric double barriers we find—depending on the asymmetry—either a simple or a composite string curve.

The transition from simple to composite is a very smooth one. In Fig. 8 we show pole string curves of the potential family $V(x) = -x^4 + ax^2 + bx$ (see Appendix A for the detailed choice of constants). When raising b while keeping one of the barrier heights constant one sees the transition from simple to composite string curve; cf. Fig. 8. For $b > 3$ ($\mu = 1$) we clearly see an additional string curve coming up. Please note that this potential—as all polynomials—is not dilatation analytic. It is known [30–33], though, that the corresponding Hamiltonians may well have stable complex eigenvalues after application of complex scaling. In a recent paper [32] we have shown that a subset of the eigenvalues of these Hamiltonians is very well approximated by

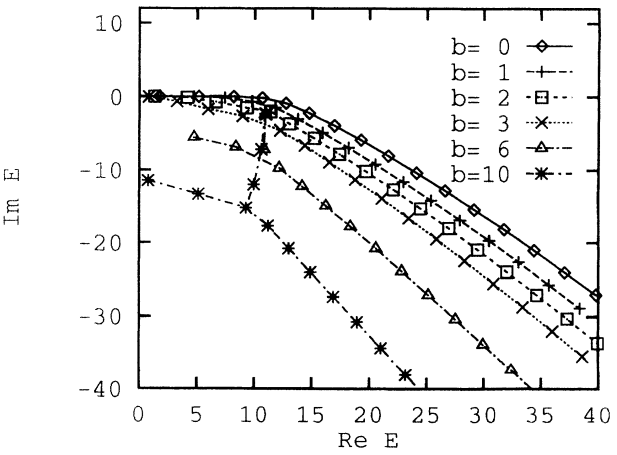

FIG. 8. The transition of simple to composite as studied with the use of $V(x) = -x^4 + ax^2 + bx$ for different parameters b. While the first three string curves are simple, the last three are composite. The eigenvalues of the first irregular part starting at the potential height are quite independent of the choice of the parameter b and the detachment point moves to lower energies when raising b. See Table VII for detailed choice of parameters.

the eigenvalues of these potentials when multiplied by a "window" function, i.e., a function that is unity inside some interval and zero outside. A possible representation is the arctangent or the error function. That is, we found in [32] that the Hamiltonians

$$H = T + V,$$
$$\widehat{H} = T + wV,$$

where w is a window function, have a common subset of eigenvalues, namely, those for which apparently the "cutting off" of the potential is irrelevant. Since the "windowed" potentials are dilatation analytic, we can use all of complex scaling and can justly speak of resonances of these "windowed" Hamiltonians. Now, since both have a common subset of complex and stable eigenvalues and what is more have identical wave functions [32] for these common eigenvalues, we argued that the original, "nonwindowed" eigenvalues can be talked of as resonances. The deeper reason for this behavior is that especially for the first resonances the eigensolutions tend to zero very quickly and therefore they depend very little on the boundary conditions far out. If one chooses the window in such a way that it stays (close to) unity in the interval where the eigensolutions are sensitive to changes (i.e., are not nearly zero) then it is immediately clear that using a window is only a *mathematical* trick, and that necessarily the eigenvalues and eigenfunctions are (nearly) identical. So, in this somewhat approximate sense, we may well speak of resonances of polynomials, especially if one bears in mind the fact that we can envisage every numerical calculation as using a window function simply because of the trivial nonexistence of a numerical infinity.

Adding another barrier to the potential does not give any new kind of pole string curve; it may well produce, though, an additional string curve (see below). We therefore introduced the concept of *irreducible units* in a recent publication [34]. There are two types of irreducible units: a single barrier (or a rather pronounced barrier), and a well and barrier(s) combination. A single barrier—as seen above—gives an irregular parts starting at the height, and a well and barrier(s) combination gives a normal string curve consisting of regular and irregular parts with a detachment point at the lowest barrier height (which, e.g., for a potential with one barrier only is the localization threshold). The assignment of irreducible units to a potential, though, is not trivial. First of all it may very well be that irreducible units overlap, like in the one-well–one-barrier combination where the barrier serves both as single barrier and as part of a well-barrier combination. Secondly, if one has more than one irreducible unit, e.g., three barriers and two wells, one cannot by inspection of the potential decide *a priori* whether the barriers are single or whether one has two barrier-well combinations.

Looking at the above description from the semiclassical point of view one observes the following. As we argue also below (Sec. VI A) the important concept is that of the *relevant* transition points. The string curve always follows (the detailed analysis in Sec. VI A shows this) approximately lines in the complex plane where for some i and j

$$\mathrm{Im}\,\alpha_{ij} = \int_{t_i}^{t_j} q(z)\,dz = 0.$$

(The more correct version, i.e., one that follows the strings up to the error of the WKB method, is shown later; for the present argument this form suffices, as we are not about to explain the "wiggly" nature of the strings.) Now the question to ask is which i and j to choose. For negative real energies, one obviously has to choose the innermost transition points, i.e., those that correspond to the classical turning points. Choosing these and evaluating the above equation, we find a line starting at the potential continuing from there with zero imaginary part. In fact, to find a numerically satisfying result we would have to include at least the next outer transition point(s) in the evaluation; as we know, $\mathrm{Im}(E) = 0$ is not the correct result even below the barrier height; what we do know, though, is that the imaginary part of the energy below the detachment point is rather small. Additionally, we are at this point only interested in the general shape of the string curve; therefore we regard the above as a good qualitative approximation. Crossing with the real energy now at least one of the barrier heights (in the more general asymmetric case) we have to include *on that side* at least another transition point. This situation had been given above when considering the composite strings of asymmetric potentials. Below zero energy the relevant transition points are the innermost. As we cross the lower one of the barrier heights we find that there are two string curves. If we concentrate on the first four transition points lying next to the origin of the complex z plane and if we number them consecutively coming from the lower barrier side (i.e., transition points 2 and 3 correspond to the classical turning points) then the regular part of the composite string can be found by setting $\mathrm{Im}\alpha_{13}$ to zero, while the irregular part starting at the potential height is due to $\mathrm{Im}\alpha_{34} = 0$. Please note that on the real energy axis α_{34} corresponds to the integral over the (higher) potential barrier, i.e., by setting $\mathrm{Im}\alpha_{34} = 0$ we look for "bound states" within a potential barrier. From the point where both string curves coalesce all four transition points are relevant (i.e., the string is "identical" to the curve $\mathrm{Im}\alpha_{14} = 0$). For higher quantum numbers we even have to include more than those four. Thus, for an asymmetric potential we have—in a certain region of the complex energy plane—an ambiguity: there are in fact two solutions, which is why we find composite strings. For symmetric potentials this possibility does not exist, which explains why we find only simple strings. So the concept of an irreducible unit emerges quite naturally also in the semiclassical approximation.

V. MULTIPLICITY OF STRING CURVES

Let us now consider the question how to find more than one string curve for a one-dimensional potential (apart

from composite strings). The simplest way of obtaining multiple strings is the following. Assume that we have two potentials $V_1(x)$ and $V_2(x)$ with the corresponding Hamiltonians and their eigenfunctions $\psi_1(x)$ and $\psi_2(x)$. Assume additionally that $\psi_1(x)$ is located in a region where $V_2(x)$ is zero and vice versa [i.e., the products $\psi_1(x)V_2(x)$ and $\psi_2(x)V_1(x)$ are identically zero]. Then the Hamiltonian

$$H = T + V_1(x) + V_2(x) \tag{6}$$

possesses two distinct (orthogonal) sets of eigenfunctions, namely, $\psi_1(x)$ and $\psi_2(x)$, so that the Hamilton matrix is block diagonal. It holds that

$$\begin{aligned} H\psi_1(x) &= T\psi_1(x) + V_1(x)\psi_1(x) + V_2(x)\psi_1(x) \\ &\equiv H_1\psi_1(x), \\ H\psi_2(x) &= T\psi_2(x) + V_1(x)\psi_2(x) + V_2(x)\psi_2(x) \\ &\equiv H_2\psi_2(x), \end{aligned} \tag{7}$$

and

$$\langle \psi_1(x) \mid H\psi_2(x) \rangle = \langle \psi_2(x) \mid H\psi_1(x) \rangle = 0. \tag{8}$$

Therefore the discrete spectrum of H is simply the union of the (discrete) spectra of H_1 and H_2

$$\sigma_d = \sigma_1 \cup \sigma_2. \tag{9}$$

Thus, in order to get more than one string curve, one possibility is to use a sum of two potentials, which are located far enough away from each other. (The "far enough," though, depends on the analytical form of the potential.) The above precondition, namely, that $\psi_1(x)V_2(x)$ and $\psi_2(x)V_1(x)$ are identically zero, is naturally very strong (too strong, one might argue). In fact, for the Hamiltonian to be nearly block diagonal it is sufficient that the corresponding mixed elements of the Hamilton matrix are sufficiently small (i.e., that the above products are only approximately zero), so that we can deal with them as a vanishing perturbation. For a concrete example, see below.

Exactly the same argument is true for potentials that have more than one barrier—or possibly barrier-well combinations—located quite far away from each other, i.e., the effect is not limited to sums of potentials. Because suppose that a Hamiltonian $H = T + V$ has the solutions $\{\psi_i(x)\}_{i=1,N}$ and there is a subset $\{\psi_i(x)\}_{i=1,m}, m < N$ that is zero outside some range which especially excludes some of the potential; then the above analysis is valid as well, only that the potential is defined piecewise

$$V(x) = \begin{cases} V_1(x), & -\infty \le x \le a, \\ V_2(x), & a \le x \le \infty. \end{cases} \tag{10}$$

(For reasons of simplicity we chose two partitions; the analysis can be trivially extended to more than two partitions.) Now we have for $i \in [1, m]$ and $-\infty \le x \le a$

$$H\psi_i = [T + V_1(x)]\,\psi_i \equiv H_1\psi_i^1(x) = E_i^1\psi_i^1(x), \tag{11}$$

where the index 1 indicates a restriction to $-\infty \le x \le a$. It can easily be extended to the whole axis by defining $V_1(x) = 0$ or $\psi_i^1(x) = 0$ for $x > a$. Another possibility would be to use the window function [32] that we proposed earlier for use with polynomial potentials; see above. Upon multiplication by the original $V(x)$ we get either $V_1(x)$ or $V_2(x)$ depending on the sign of the argument of the arctangent.

Then the Hamiltonians H_1 and H_2 are defined on the whole axis and have eigenvalues E_i^1 or E_i^2, respectively, as indicated above. So again the Hamilton matrix is block diagonal and the discrete spectrum of the complete Hamiltonian is the union of the (discrete) spectra of H_1 and H_2 provided that for all wave functions $\psi_i^1(x)$ and $\psi_i^2(x)$ it is true that

$$V_2(x)\psi_i^1(x) = V_1(x)\psi_i^2(x) = 0. \tag{12}$$

(And if this condition is only approximately valid then we will find almost exact block separability, etc.; see above). In Fig. 9 we show an example of this behavior. This potential

$$V(x) = V_0 \cos(ax)e^{-bx} \tag{13}$$

(in the figure we used $V_0 = 20$, $a = 1$, $b = 0.15$, and $\mu = 1$) features four to five overlapping barrier-well combinations that are independent of each other, as we have recently shown [34] by comparing the union of the spectra of the "reduced" Hamiltonians with the complete Hamiltonian.

Indeed we have not found a single counterexample to this behavior. Even in situations where one might be led to believe that there should be more than one string curve one may not find them. For example, if one considers a potential with two different thresholds, as in a chemical reaction with intermediate species, one is tempted to believe in two distinct channels each having their "own" string curve. As can be seen in Fig. 10 this is definitely not true. We do find two continua at the threshold val-

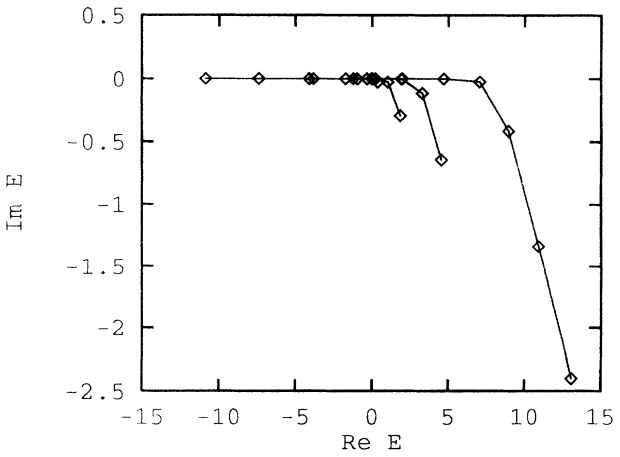

FIG. 9. Pole string curves of $V(x) = 20\cos(x)e^{-0.15x}$ ($\mu = 1$). There are at least three string curves visible in the plot. These correspond to irreducible units that consist of a well plus the adjacent barriers. See text for further details.

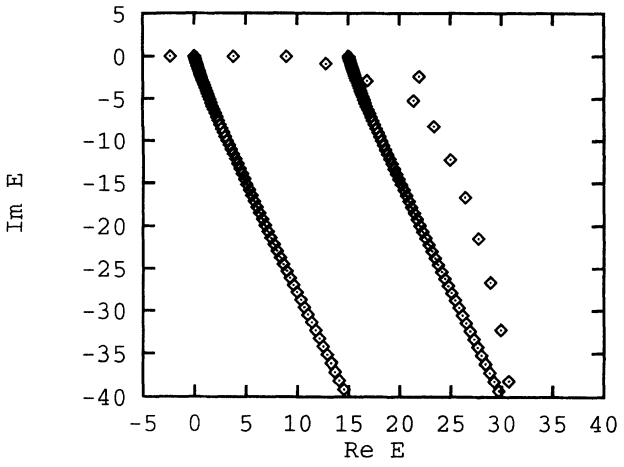

FIG. 10. Pole string curve of piecewise defined potential—Eq. (A8)—with two different thresholds (one at zero, one at 15 hartree). Note that first there is one string curve only and secondly this string curve is just as was to be expected, i.e., it is a composite string curve showing no irregularities because of the additional threshold. Plotted also in the figure are the two discretized cuts starting at the thresholds.

ues, but there is only one string curve.

This means that one can envisage—as we have already mentioned above—a given potential as being composed of "irreducible" units in the sense that *one irreducible unit is the source for one string curve.* As we have seen in the last examples the irreducible units are not necessarily disjoint intervals. Usually they consist of a well together with a "minimal" environment, i.e., the surrounding barriers.

The above findings are not astonishing in the sense that obviously when there is more than one string curve there is a "hidden" symmetry in the form of an additional quantum number within the system. Surprising, however, is the fact that one can correlate this quantum number with an irreducible unit and that there seem to be no wave functions $\psi(\eta x)$ (i.e., after the CSM transformation) which are delocalized over the whole potential. It may seem appropriate to mention again that finding mostly single string curves is a typical property of the *one-dimensional* Schrödinger equation. Already in two dimensions the situation is completely reversed in the sense that one does not observe single string curves readily, because of the additional degrees of freedom.

VI. ABOUT WIGGLES

Potential string curves with wiggly behavior have been reported first by Rittby *et al.* [12–14]. This behavior has caused considerable discussion, since Korsch *et al.* [26] questioned the existence of wiggles. Their doubts were based on calculations using the complex rotated Milne method [35] and on semiclassical calculations [26], which gave essentially the same results.

Recently, though, Andersson [27] was able to show that WKB calculations give the correct results, if one includes enough transition points. He was able to verify the results of Rittby *et al.* using a first order phase integral approximation, but including four transition points. The results of Rittby *et al.* have also been confirmed by other authors using different methods. Using the complex scaled Fourier grid Hamiltonian method [31], we were able to achieve at least six digits of agreement.

One must conclude therefore that wiggles are not numerical artefacts, though their interpretation is somewhat unclear. The following should be noted.

(i) In all cases wiggles occur after the localization threshold so the oscillatory tail of the string curve contributes (after "backrotation") to the (measurable) background at most [36].

(ii) "Resonances" constituting the wiggly tail are not localized within the attractive region of the potential, so the process underlying these eigenvalues is obviously not tunneling. The real nature, though, is unclear.

(iii) The question of wiggly or nonwiggly cannot be correlated with potential parameters. Rather it depends on the analytical structure of the potential; see below.

(iv) The WKB analysis [27] shows that one has to use more than one pair of transition points to calculate the correct eigenvalues. Additionally Andersson [27] has shown—see also Sec. II above—that those transition points that on the real axis correspond to the classical turning points completely lose their importance. [A short word of explanation: For (real) energies below the potential height one has in this double barrier case four transition points on the real axis. Going higher with the energy one finds those zeros moved into the complex plane in four different quadrants. Additionally there are also "new" complex roots in every quadrant. The latter have no analog on the real axis; they exist because of the analytical structure of the potential *in the complex plane.*] Since those transition points that are necessary for the correct results have no "analog" on the real axis the wiggles seem to be a feature of the complex plane only, i.e., their existence is due to the analytical continuation.

Generally speaking, wiggles seem to be an effect due to the *complex* potential (i.e., its analytical continuation) and less due to the potential itself; see below. Nevertheless wiggles are a very interesting analytical phenomenon, and it is fascinating to look into that matter, because it shows the complexity of the analytically continued Hamiltonian.

Another word of warning may seem appropriate. Wiggles are hard to find in the sense that when employing a basis set method—even such a good one as the Fourier grid Hamiltonian method [31]—and using, e.g., too small values of the integration range or the basis set size one may end up with resonance string curves where the last resonances seem to be stable enough, but the string curve is smooth. Upon enlarging the basis set size, though, we found that wiggles appear (data not shown). The key is the stability of the eigenvalues with respect to variation of θ; one should use a rather strict condition (e.g., constancy of the eigenvalues to at least three digits upon variation of θ and integration range). If one finds wiggles, though, our experience is that they can be trusted. We have found no example where with low accuracy we

found wiggles and with high accuracy found none. In order to be absolutely sure whether there are no wiggles one should use a direct numerical integration scheme at the found eigenvalues (with a very small step size). We rechecked our results when in doubt using a renormalized Numerov or a log-derivative method [37–39].

Basically, we checked three different classes of potentials. (1) $P(x)$ with uneven order or negative leading coefficient, (2) $P(x)e^{-cx}$, and (3) $P(x)e^{-cx^2}$, where $P(x)$ is a polynomial. Specifically, we checked polynomials up to fourth order, because we had the impression that no new insight was gained by going to still higher orders. As mentioned above, we also checked damped periodic potentials, but, since those are dilatation analytic in a comparatively small portion of the complex plane only, we have not even seen a localization threshold for the parameters we chose. The same is true for potentials that have a polynomial in the exponent of order greater than 2: those are dilatation analytic only for angles

$$\theta < \theta_{\max} = \frac{2\pi}{n},$$

where n is the order of the polynomial in the exponential. After this angle $\theta_{\max}$ the sign of the real part of $z^n = e^{in\theta}x^n$ changes and the potential diverges exponentially. Usually, though, we need the better part of the fourth quadrant to include a portion of the spectrum that is large enough to decide whether it belongs to the smooth or the wiggly type.

Wiggles never occur before the localization threshold; in fact, we tend to argue in the following way. Consider the string curve as a function $\mathrm{Im}(E)$ vs $\mathrm{Re}(E)$. Then the "spikes" are local minima surrounded by local maxima. The first local maximum is always the localization threshold, so very naturally there are no wiggles before the latter. Pure polynomials therefore "cannot" have any wiggles, because they do not have a localization threshold. In the case of the symmetric potential $V(x) = ax^4 + bx^2$ the WKB ansatz for resonances can be solved analytically [40] in terms of elliptic functions [41]. It can be verified in this case that the potential—or the corresponding Hamiltonian—has no localization threshold at all.

We are left with two of the above mentioned classes of potentials. As far as we can say, the class 2 (exponential) has wiggles for no parameters or polynomials while class 3 has wiggles for all parameters and polynomials. Even for $n = 0$ (simple Gaussian barrier) we found wiggles, though only for rather high imaginary energies. It seems that wiggles are an effect specific to the "Gaussian" (e^{-x^2}) type of long range part of the potentials.

A. A semiclassical analysis

In this paragraph we shall analyze the situation from a semiclassical point of view. In order to find the possible cause for the wiggly nature of the spectrum we will here concentrate on two potentials, namely, the potential used by Rittby *et al.* [12–14],

$$V_1(x) = (\tfrac{1}{2}x^2 - 0.8)e^{-0.1x^2} + 0.8,$$

which was first used by Moiseyev, Certain, and Weinhold [42], and the one called the Bain potential first used by Bain, Bardsley, Junker, and Sukumar [43],

$$V_2(x) = 7.5x^2e^{-x}.$$

Both potentials are symmetric and therefore the transition points (tp) that are necessary for the semiclassical calculations lie point symmetrically with respect to the origin. As Andersson [27] has already remarked, of those one needs to include only the ones in the first quadrant of the complex energy plane. The integrals needed are then

$$\alpha_{ij} = \int_{t_i}^{t_j} q(z)dz, \qquad i,j \in [0,1,\ldots]. \tag{14}$$

In the above formula we have defined the origin to be t_0. The WKB conditions for complex energy resonances can then be derived as [27]

$$2\alpha_{01} = (n + \tfrac{1}{2})\pi \quad \text{for 1 tp}, \tag{15}$$

$$2\alpha_{01} - i\ln(1 + e^{2i\alpha_{12}}) = (n + \tfrac{1}{2})\pi \quad \text{for 2 tp}. \tag{16}$$

Formula (15) can be used up to a few quantum numbers (three for mass 1 a.u.) after the localization threshold in the case of V_1 and for the whole spectrum in the case of V_2.

As is known from the analysis of Andersson [27] the Hamiltonian corresponding to V_1 shows wiggles also in the semiclassical approximation if (and if only) one includes more than two transition points. In fact, in order to get a good approximation to the whole known string one needs five transition points (considering symmetry). But looking at Andersson's results, one observes that the main *qualitative* correction is the inclusion of the second transition point. Let us therefore take a closer look at condition (16), but with a slight modification. We will now consider string curves instead of strings, i.e., the left hand side of Eq. (16) is required to be real (instead of half-integer multiples of π). Rearranging Eq. (16) we get

$$\begin{aligned} 2\alpha_{01} - i\ln\left(1 + e^{2i\alpha_{12}}\right) &\in \mathbb{R} \\ &= -i\ln e^{2i\alpha_{01}} - i\ln\left(1 + e^{2i\alpha_{12}}\right) \\ &= -i\ln\left[e^{2i\alpha_{01}}\left(1 + e^{2i\alpha_{12}}\right)\right]. \end{aligned} \tag{17}$$

Since the latter must be real, the real part of the logarithm must vanish. Since now ($z = |z|e^{i\beta}$)

$$\ln z = \ln|z| + i(\beta + 2n\pi),$$

condition (17) can be rewritten as

$$1 = |e^{2i\alpha_{01}}\left(1 + e^{2i\alpha_{12}}\right)| = |e^{2i\alpha_{01}}\left(1 + e^{2i\alpha_{12}}\right)|^2,$$

$$1 = e^{-2\mathrm{Im}(\alpha_{01})}[1 + 2e^{-\mathrm{Im}(\alpha_{12})}\cos(\mathrm{Re}\,\alpha_{12}) + e^{-2\mathrm{Im}(\alpha_{12})}] \tag{18}$$

$$= e^{-2\mathrm{Im}(\alpha_{01})} + 2e^{-\mathrm{Im}(\alpha_{01})-\mathrm{Im}(\alpha_{02})}\cos(\mathrm{Re}\,\alpha_{12}) + e^{-2\mathrm{Im}(\alpha_{02})}, \tag{19}$$

where the last equality follows from $\alpha_{02} = \alpha_{01} + \alpha_{12}$ (though when calculating this integral one has to be careful to choose a path through the complex plane that does not cross any cut; numerically we employ the equation $\alpha_{02} = \alpha_{01} + \alpha_{12}$ in order to avoid crossing any cut). For convenience we will define the square bracket of Eq. (18) to be a function β.

Now we have three imaginary parts of integrals that are of interest, namely, those of α_{01}, α_{12}, and α_{02}. In Fig. 11 we show the exact resonances of V_1 together with the lines where the imaginary part of the mentioned integrals (and additionally that of α_{03} and α_{23}) vanish together with the signs of those integrals to the right and left of the corresponding line.

One observes the following. In the first part of the string (up to the first wiggle) the imaginary part of α_{12} (and also that of α_{23}) is positive. Therefore *the only way to fulfill condition (18) is that* $\mathrm{Im}(\alpha_{01}) = 0$. This may need some explanation.

Let us look at the portion of the complex energy plane that is defined by

$$\{E \,|\, \mathrm{Re}(E) > 0\,;\, 0 > \mathrm{Im}(E) > z_{12}(E)\}\,,$$

where $z_{12}(E)$ is the line defined by $\mathrm{Im}(\alpha_{12}) = -\ln 2$. Here the latter is growing monotonically in the direction of the real energy axis. We are faced with three possibilities: $\mathrm{Im}(\alpha_{01})$ is negative, zero, or positive. If it were (significantly) positive [so the string would deviate significantly from the line $\mathrm{Im}(\alpha_{01}) = 0$] then β would have to be large compared to unity. This could be achieved only when $\mathrm{Im}(\alpha_{12}) < 0$, which (see Fig. 11) is a contradiction. Now if $\mathrm{Im}(\alpha_{01})$ is (again significantly) negative then β should be close to zero. The function β has only one zero, namely, for $\mathrm{Im}(\alpha_{12}) = 0$ and $\mathrm{Re}(\alpha_{12}) = \pi$. *This condition is fulfilled for the resonances constituting the first wiggle*, as can partly be seen in Fig. 11. Andersson had already observed [44] that the wiggles come close to positions where

$$\sum_{j=m+1}^{m+n} e^{2i\alpha_{mj}} = -1$$

and he called them *total transmission solutions.* Please observe also that the position of the spikes will depend on the mass, although (a) neither of the lines in the figure depends on the mass and (b) we are considering string curves (as opposed to strings). The reason is simply that the actual value of $\mathrm{Re}(\alpha_{12})$ is part of the condition. Since this is mass dependent, the position of the spike will be also; a fact that will be confirmed later in this contribution.

Now, if $\mathrm{Re}(\alpha_{12})$ is not an (odd) integer multiple of π, the only possibility left to fulfill condition (18) is that $\mathrm{Im}(\alpha_{01})$ is identical to zero. (To be more exact: it must be very small.) So the eigenvalues are distributed along the line $\mathrm{Im}(\alpha_{01}) = 0$ until the resonances get nearer to $z_{12}(E)$, where one can observe the first deviation of the real string from the above line [$|\mathrm{Im}(\alpha_{12})|$ grows rapidly on either side of its zero, so z_{12} is very near the zero line.] If now one crosses z_{12} then the function β is larger than unity [independent of the value of $\mathrm{Re}(\alpha_{12})$; z_{12} was chosen so that even for $\mathrm{Re}(\alpha_{12}) = \pi\beta > 1$; for other values we could have chosen a line that is even closer to $\mathrm{Im}(\alpha_{12}) = 0$]. This means that—in order to fulfill condition (18)—the string must (a) deviate from the line $\mathrm{Im}(\alpha_{01}) = 0$ into (b) that portion of the complex energy plane where $\mathrm{Im}(\alpha_{01}) > 0$. This is exactly what one observes; see Fig. 11.

Looking now at the next portion of the string one sees that it follows—more or less—the line $\mathrm{Im}(\alpha_{02}) = 0$. This is clear, because a very similar analysis to the above can be made now considering also $\mathrm{Im}(\alpha_{23})$ and $\mathrm{Re}(\alpha_{23})$. We have more possibilities in this case, so that the next wiggle does not have to occur when $\mathrm{Im}(\alpha_{23}) = 0$ [one finds, though, that $\mathrm{Re}(\alpha_{23})$ is again an odd integer multiple of π at the next "spike" and that $\mathrm{Re}(\alpha_{23})$ is very small]. Please observe that the string is not

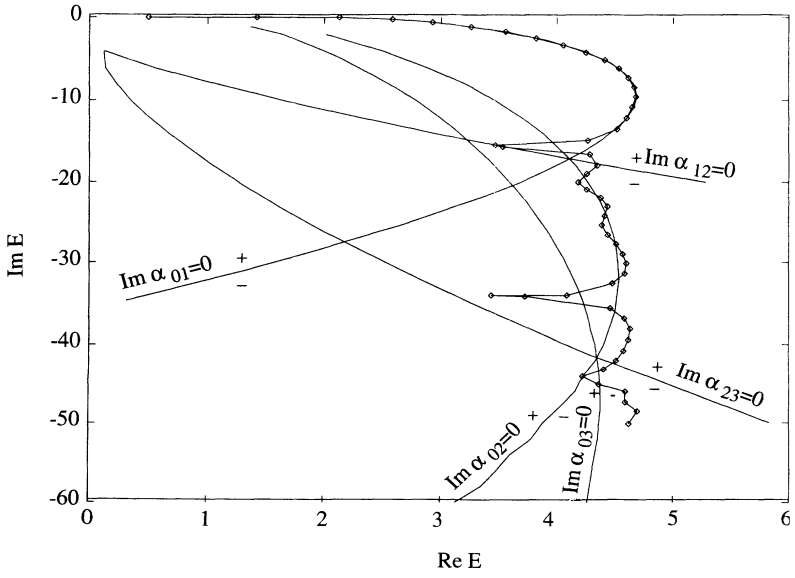

FIG. 11. Resonances of the potential $V(x) = (1/2x^2 - 0.8)e^{-0.1x^2} + 0.8$ for $\mu = 1$. Additionally plotted are the lines on which the imaginary parts of the indicated α_{ij} vanish. The corresponding sign change (+ and −) is also indicated. See text for details.

smooth, because $\mathrm{Im}(\alpha_{03})$ is not that large in that region. One sees from Andersson's results [27] that one needs to include the third transition point already after very few quantum numbers in order not to deviate too much from the correct results. After crossing the line $\mathrm{Im}(\alpha_{23}) = 0$ the string again deviates significantly from the line $\mathrm{Im}(\alpha_{03}) = 0$, just as before it had deviated from $\mathrm{Im}(\alpha_{02}) = 0$ when crossing $\mathrm{Im}(\alpha_{12}) = 0$.

Thus, from the semiclassical point of view, the situation is quite clear. The string cannot be smooth and tending back to zero real energy, because first of all we are crossing the line $\mathrm{Im}(\alpha_{12}) = 0$ and then there is an "interference" between $\mathrm{Im}(\alpha_{02})$ and $\mathrm{Im}(\alpha_{03})$ ("interference" meaning that the order of magnitudes are such that none can be neglected). The latter is the cause also for the mass dependence of this part of the string curve, as we mentioned above.

Now let us turn to the Bain potential. What is different here that prevents a mechanism similar to the above? The answer is very simple (although astonishing): There is no line $\mathrm{Im}(\alpha_{12}) = 0$. $\mathrm{Im}(\alpha_{12})$ is positive definite. It does have a minimum, as can be computed, but no zero. Therefore the only possibility to fulfill condition (18) is $\mathrm{Im}(\alpha_{01}) = 0$ and this gives a smooth mass-independent string curve, without any spikes.

The reason for this behavior can be tracked down to the distribution of the transition points of the corresponding potentials. Let us look at the function $\mathrm{Im}(\alpha)$ quite generally. The first transition point has the coordinates $(a + ib)$ and the next $(a' + ib')$ with $a' > a$ and $b' > b$ in the complex z plane ($z = x + iy$). As the function $q(z)$ under the integral has no singularities in the interval, we may choose a straight line $y = mx + b$ as integration contour as long as we do not cross any cut, which is always true when integrating between adjacent transition points. Then

$$\mathrm{Im}(\alpha) \;=\; \int_a^{a'} |q[x(1+im)+ib]|\,(m\cos\phi + \sin\phi)\;dx.$$

Now we are performing the integration *outward*, i.e., we are moving in a positive x direction. Therefore the real part of q must be positive. This restricts us to $-\pi/2 \le \phi(z) \le \pi/2$, which in the complex $E - V(z)$ plane means that the argument of $E - V(z)$ is between $-\pi$ and π (so the whole plane is still available).

Since $|q|$ is a positive function with no zero in the interval under observation the condition $\mathrm{Im}(\alpha) = 0$ implies that

$$\int_a^{a'} m\cos\phi + \sin\phi\,dx \;=\; 0.$$

Now let us approximate $\phi(x) = -Cx$ [numerical experiments show that this is a good approximation especially between the "outer" zeros, i.e., those further into the complex z plane; in fact, the only property we need is that $\phi(x)$ is a strictly monotonic function):

$$\begin{aligned} 0 &= \int_{\phi(a')}^{\phi(a)} m\cos\phi + \sin\phi\,d\phi \\ &= m\{\sin[\phi(a)] - \sin[\phi(a')]\} + \cos[\phi(a')] - \cos[\phi(a)] \\ &= 2m\cos\left(\frac{\phi(a)+\phi(a')}{2}\right) + 2\sin\left(\frac{\phi(a)+\phi(a')}{2}\right). \end{aligned}$$

Now let $\phi(a) = \phi(a') + b$ where b ($0 \le b \le \pi/2$) is some constant. It follows that

$$-m \;=\; \tan\left(\phi(a') + \frac{b}{2}\right).$$

As m is positive this restricts $\phi(a') + \frac{b}{2}$ to be smaller than zero. One observes that between every two zeros of $E - V(z)$ lies one of $\mathrm{Re}(E - V)$ or $\mathrm{Im}(E - V)$, which means that since

$$E - V(z) \;=\; |E - V(z)|e^{2i\phi(z)}$$

$2\phi(a)$ must differ from $2\phi(a')$ by at least $\pi/2$. Therefore $b > \pi/4$. Consequently, one has a maximal m, namely, $\tan(3\pi/8) \approx 2.41$. Values of m greater than this will quite generally lead to $\mathrm{Im}(\alpha) > 0$. [Please note that if $2\phi(a)$ should have to differ from $2\phi(a')$ by at least π then the maximal m is 1.]

Upon checking the distribution of zeros for the above potentials one finds that for the potential $V_1(x)$ this poses no problem at all. For all resonance energies the value of m for all of the different α's is well below 2, so that we can find everywhere $\mathrm{Im}(\alpha) = 0$. We have shown that before. But, turning now to $V_2(z)$, we find that only the first zero obeys the above restriction. This means very generally that, e.g., $\mathrm{Im}(\alpha_{12})$ is always positive, as we have already mentioned above.

Please let us stress the fact that the condition $m < \tan(3\pi/8)$ has been derived under very general conditions and is therefore valid for every potential, i.e., whenever the slope between two consecutive zeros in the first quadrant of the complex z plane is larger than the above value the corresponding $\mathrm{Im}(\alpha)$ is strictly positive.

B. The transition from wiggly to smooth

We studied the transition from wiggly to smooth behavior with the help of the potential class

$$V(x) \;=\; 70(0.5x^2 - 0.08)e^{-ax-bx^2} \qquad (20)$$

and varied a and b ($\mu = 0.7$). In the limit $b = 0$ we end up with a variant of the Bain potential [43] and in the limit of $a = 0$ we have a potential that is similar to the one used by Rittby *et al.* [13]. While the first does not show any wiggles, the second one does, as we mentioned above. As can be concluded graphically in Fig. 12 the transition is very smooth. There is no breakdown at some quotient of a and b. Those eigenvalues that constitute the "spikes" simply melt smoothly into the string curve. Note, though, that all of the shown strings are "wiggly;" only the spikes are not that prominent for large a. We might conclude from this—as can be seen also from Andersson's [27] and the above semiclassical

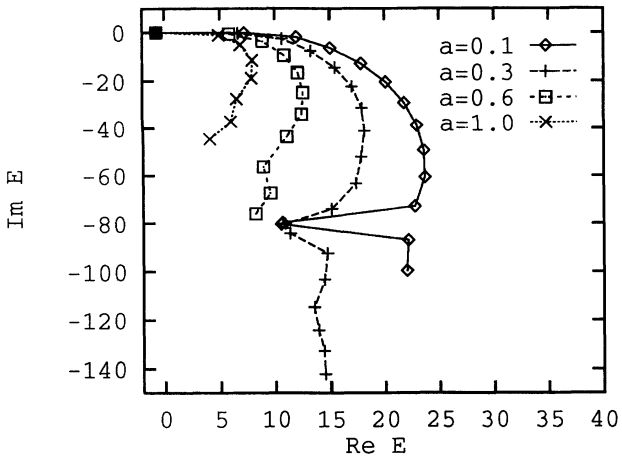

FIG. 12. The transition from wiggly to smooth for potential $V(x) = 70(0.5x^2 - 0.08)e^{-ax-bx^2}$; Table VIII below for the detailed choice of constants. As shown in the figure the spike simply melts smoothly into the string curve. There is no breakdown of any sort visible, neither have we found one when changing the parameters in other different ways.

analysis—that the behavior of the "tail" of the potential (i.e. far out) is important for the wiggles. Since this tail is not affected very much by a—if not chosen too large with respect to b—we find such a smooth transition. Accepting the validity of the semiclassical approximation, the reason for this smooth transition is the distribution of the zeros or rather their dependence on a. That is, since the Gaussian term e^{-bx^2} starts to behave rather violently around $y = ix$, i.e., $m = 1$, we find that even for large a the zeros are distributed along or near that line. This means that m is smaller than the critical value of $\tan(3\pi/8)$ and therefore we can have wiggles. We found that the slope between transition points 2 and 3 (constituting α_{23}) is smaller than $\tan(3\pi/8)$ as long as a/b is smaller than ≈ 100. For larger values of a/b there can be no wiggles but only a smooth string.

C. The dependence on mass and barrier thickness

Let us turn now to look at the wiggles explicitly for a specific example. Let us choose the family

$$V(x) = (ax^2 + bx + c)e^{-dx^2}$$

with $b = 0$ for the moment (symmetric case). The choice is completely arbitrary in the sense that we could have chosen another family to find basically the same results. The family we have chosen here is just very convenient numerically.

Rittby *et al.* have calculated the spectrum for this kind of potential for different d [13] and found an increase of the "frequency" of the wiggles for increasing d. By changing d only one alters the "strength" of the potential, i.e., the barrier thickness and the height, and the position of the maxima. If one changes the thickness only one has to change both a and d. This amounts to a (real) dilatation of the coordinate and is equivalent to changing the mass (one is reminded of the well-known concept of mass weighted coordinates). In the following we will therefore write "mass-thickness."

As can be seen from Fig. 2 this variation of parameters also changes the wiggles. The rest of the string curve (i.e., the part before the localization threshold) is not affected by this transformation. This is clear, since—as mentioned above—changing the thickness is equivalent to changing the mass and we showed earlier that the regular part of a string curve does not depend on the mass—to first order. As can be seen also from Fig. 2 the frequency of the oscillations is not affected by changing the mass.

That the irregular part of the string curve is nevertheless affected by the mass may seem surprising, since the regular is not. We showed in Sec. II that one can understand the nondependence of the string curve on the mass in terms of Eq. (1). Obviously, if this formula holds the string curve cannot depend on the mass. But, as we showed in some detail above, the irregular part for these kinds of potential is governed by an "interference" of more than one transition point. For example, consider two pairs of transition points. The corresponding generalization of Eq. (1) is [27]

$$2\alpha_{01} - i\ln\left(1 + e^{2i\alpha_{12}}\right) \in \mathbb{R}. \tag{21}$$

One observes that Eq. (21) depends nontrivially on the mass; therefore the corresponding string curve is mass dependent. Additionally, as we showed above, the "spikes" occur at or near points where the lines $\mathrm{Re}\alpha_{ij} = (2n+1)\pi$ *and* $\mathrm{Im}\alpha_{ij} = 0$ (ij is, e.g., 12 for the first spike). While the position in the complex plane of the former depends on the mass, the latter does not. Therefore the frequency of the wiggles will not alter, but the position can. Whether the position of the spikes alters or not rather depends on the curvature of the lines $\mathrm{Re}\alpha_{ij} = (2n+1)\pi$.

D. The "frequency" of the oscillations

If we now keep the thickness constant, but change the height of the potential (keeping the depth constant as Rittby *et al.* did), we find that this affects the frequency of the wiggles. In Fig. 13 this is depicted. For decreasing height the frequency of the oscillations grows rapidly until for nearly zero height there are no resonances at all, but only bound states (the arrow in Fig. 13 indicates a single bound state for a set of parameters such that the potential height is 0.0064 hartree).

The same can be concluded from a different set of calculations where we kept the total height (height minus depth) of the potential constant and altered the quotient (height)/(depth). We find (see Fig. 14) again a drastic increase of the frequency especially for small values of the height.

We conclude that the potential height is responsible for the frequency of the wiggles (within a family). The potential depth seems to play no role, which is consistent with our previous remark that wiggles seem to depend rather on the "tail" of the potential.

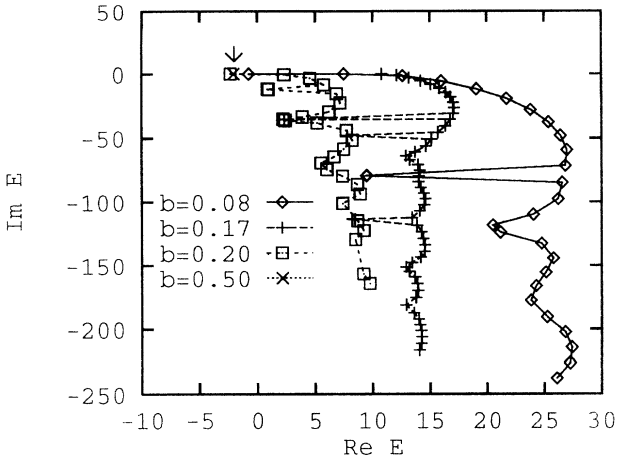

FIG. 13. Pole string curves for $V(x) = a(0.5x^2 - b)e^{-cx^2}$ with constant potential depth ($\mu = 0.7$). As can be seen from the figure the "frequency" of the wiggles increases rapidly with lowering of the potential height above the threshold.

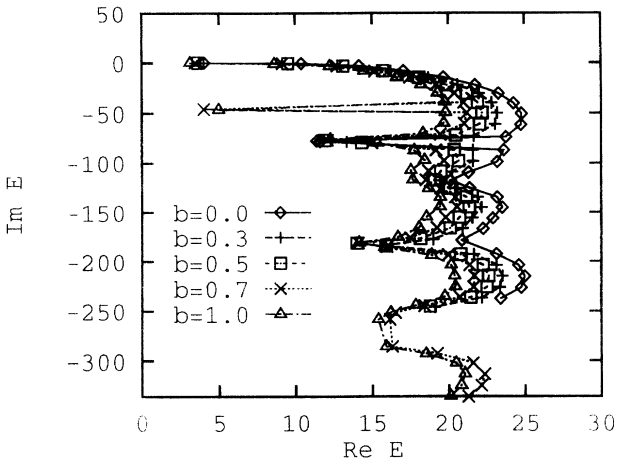

FIG. 15. Pole string curves of asymmetric $V(x) = a(4x^2 - bx)e^{-cx^2}$ for different values of "asymmetry." The detachment points (this cannot be seen in the figure) become lower with lowering of one of the barriers; they are in fact identical with the smallest barrier height. As can be seen, the position of the "spikes" is constant over a whole range of b. Only one more spike might be added eventually, if the localization threshold gets lower than the position of that "virtual" spike.

E. The position of the "spikes"

Let us now turn to the question of what parameters affect the position of the spikes on the imaginary energy axis. To gain insight into this point it is instructive to look at the asymmetric case ($b \neq 0$) of the above mentioned potential family. We kept constant the height of one of the barriers while lowering the other one. (According to our observations the change in position of the maxima is not important; data not shown.)

In Fig. 15 we show this asymmetric case. The outermost string curve corresponds to the symmetric case ($b = 0$) and the string curves from right to left correspond to a diminishing left barrier (see Appendix A for the detailed choice of constants). One sees beautifully that (for the same thickness-mass) the positions of the spikes are constant within a certain range of the parameter b. If one lowers the second barrier further one simply gets an additional spike. As one can see in the figure this happens rather discontinuously. This behavior may be called surprising, if one bears in mind that changing the height affects the frequency of the wiggles. It seems that in order to increase the frequency of the oscillations both barriers have to be lowered. Please note that (not

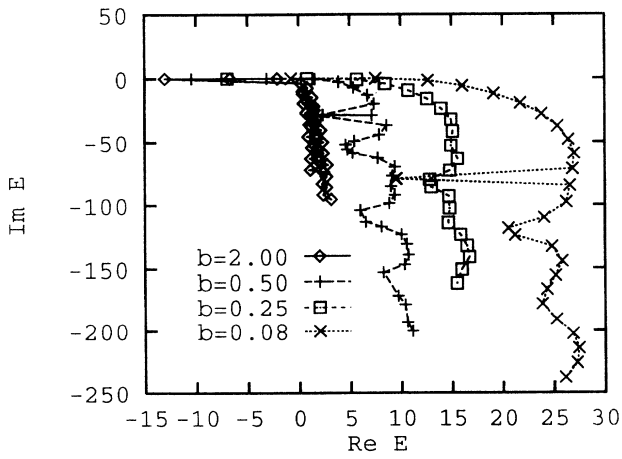

FIG. 14. Pole string curves for $V(x) = a(0.5x^2 - b)e^{-cx^2}$ with constant total height (height above threshold minus depth); the quotient of height above zero and depth is changed. Note the very similar behavior as in Fig. 13, indicating that the frequency of the oscillations depends indeed on the potential height (the mass was 0.7 here).

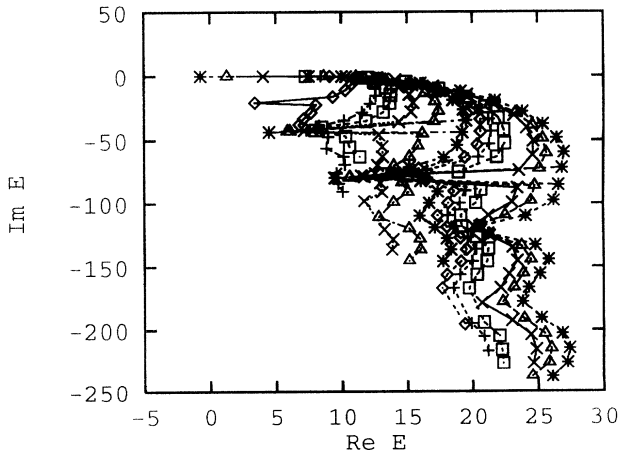

FIG. 16. Pole string curves for $V(x) = a(0.5x^2 - b)e^{-cx^2}$ with constant height. Due to the change in the parameters the barrier maxima get closer when the potential depth is raised; in the end there is only one barrier left. This case corresponds to the innermost string curve, which has an irregular part only. Note also essentially the same behavior as in Fig. 15. (See Tabie III below for the choice of constants a and b. The innermost string corresponds to the first line in the table, etc.)

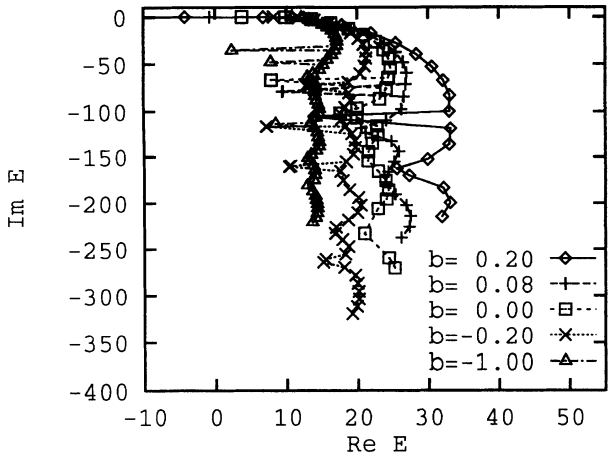

FIG. 17. Pole string curves for $V(x) = a(0.5x^2 - b)e^{-cx^2}$ with constant height and constant position of maxima. As can be seen in the figure the positions of the spikes are not constant, so that it should be concluded that the positions are a function of mass-thickness only.

easily seen in the figure) the detachment point is always the lower one of the two barrier heights.

Keeping constant the height and altering the depth, one gets essentially the same picture as can be seen in Fig. 16. Again we find that the positions of the spikes are constant over a large region of parameters and then there is another spike added while the rest remain unchanged. Note that this analysis is valid only for constant mass-thickness. If one, for example, also alters the parameter d such that the positions of the maxima are constant, one does not get this feature; see Fig. 17.

We conclude that the positions of the spikes—within a potential family—depend on the mass-thickness only. It might be the case, though, that some spikes are "missing," because the localization threshold lies below them (with respect to the imaginary part of the energy).

The reason for this behavior can again be tracked down (accepting the validity of the semiclassical approximation) to the dependency of the lines $\mathrm{Im}\alpha_{ij} = 0$ and $\mathrm{Re}\alpha_{ij} = (2n+1)\pi$. One finds numerically that the latter (e.g., $\mathrm{Re}\alpha_{12}$) do depend very little on the potential parameters. In fact, the higher ij the less they depend on the potential. Even doubling the potential height does not alter them significantly. They do depend, though, on the mass. Additionally these lines are almost parallel to the real energy axis. Therefore, when mass-thickness is changed then the possible positions of the spikes are altered significantly. When we are changing the other parameters of the potential, we change the slope and position of the lines $\mathrm{Im}\alpha_{ij} = 0$, but, since the lines $\mathrm{Re}\alpha_{ij} = (2n+1)\pi$ are almost parallel to the real energy axis, the position of the spikes, i.e., the imaginary energy where those spikes occur, is almost invariant.

VII. SUMMARY

Let us now summarize our findings, which were in this contribution based mostly on three different types of one-dimensional potentials, namely, the pure polynomials, polynomial times exponential, and polynomial times Gaussian damping.

For the phenomenological description of resonance string curves we introduced qualitatively the concept of irreducible units of a one-dimensional potential and that of regular and irregular parts of the string curve of resonances. There are two different types of units, namely a single barrier and a barrier-well combination (or one well plus surrounding barriers). These two have different spectra, namely, the first one gives an irregular string curve starting at the potential height, while the second gives a normal string curve with both regular and irregular parts. A potential consisting of more than one irreducible unit will have multiple or composite (or both) string curves. The concept of irreducible units amounts to the introduction of a quantum number that labels those units. The assignment of a combined index (n, m), where n is the irreducible unit and m numbers the resonances within the subset, gives a unique way of labeling the complex energy eigenvalues. Please note that we have not found a single example where this assignment was impossible, i.e., where the resonant state was delocalized over two or more wells.

While the physical interpretation of the eigenvalues of the regular part of a string curve is quite obvious, that of the eigenvalues constituting the irregular part needs some more work to be spent on it. In the case of wiggles we mentioned some points concerning this question. Putting together the results of Andersson [27,44] and our own analysis seems to point in the direction that for wiggles the analytic continuation of the potential to the complex coordinate plane seems to play a major role. One of the problems that we have with those states is that they are not localized in the attractive region of the potential, but rather beneath it. We showed briefly that the localization pattern changes at the localization threshold from being localized within the barriers (although with real energy far above them) to being localized outside.

Our presented numerical results give evidence for the fact that the regular part of the string curve is always a very smooth curve that has two important points: the detachment point and the localization threshold. We briefly mentioned without going into detail that the detachment point coincides with the lowest relevant barrier height. Relevant means here that this barrier must be part of the irreducible unit that gives that particular string curve.

We have also dealt to some extent with the question of the mass dependence of the string curves. We found that the regular part above V_0 does not depend on the mass. This fact—as we showed—is consistent with the first order phase integral approximation [17], if (and only if) it suffices to include one transition point only. If—as in the case of the wiggles—one has to use more than one pair of transition points the string curve will depend on the mass-thickness. Or, to turn this statement around, whenever we find that a portion of the string curve depends on the mass, we cannot expect to explain the results using a one turning point WKB analysis. In this formulation our result may be interpreted as a strong support of Andersson's findings [27].

Besides mentioning a few points on the interpretation of wiggles we presented a semiclassical analysis showing that from a semiclassical point of view the string of the potential used by Rittby *et al.* [$V(x) = (0.5x^2 - 0.8)e^{-0.1x^2} + 0.8$] necessarily has wiggles. We showed that—at least qualitatively—the spectrum of the corresponding Hamiltonian can be understood by inspecting lines in the complex energy plane, where for some i and j

$$\mathrm{Im}\,\alpha_{ij} = \int_{t_i}^{t_j} q(z)\,dz = 0.$$

The string quite generally follows lines on which $\mathrm{Im}\,\alpha_{0j}$ is zero until one crosses a line where $\mathrm{Im}\,\alpha_{jj+1} = 0$. The wiggles are due to the "interference" between, e.g., $\mathrm{Im}\,\alpha_{0j}$ and $\mathrm{Im}\,\alpha_{0j+1}$ and spikes occur where $\mathrm{Re}\,\alpha_{jj+1} = n\pi$ and $\mathrm{Im}\,\alpha_{jj+1} = 0$. Numerical experiment revealed that for potentials other than the above (but of the type polynomial times Gaussian damping) the situation is the same. We conclude therefore that one can indeed "understand" the spectrum of the complex scaled Hamiltonian in those terms.

We also gave a reason for the absence of wiggle when using potentials of the type polynomial times exponential damping. In fact, we were able to show that for $\mathrm{Im}\,\alpha_{ij}$ to be zero the slope between the corresponding transition points i and j must not exceed the value of $\tan(3\pi/8)$. If it does then $\mathrm{Im}\,\alpha_{ij}$ is positive definite. This is exactly the case for all but the innermost zeros of the Bain potential [43] [$V(x) = 7.5x^2e^{-x}$], which is why the corresponding Hamiltonian has a smooth string and no wiggles. Let us mention that we have made no assumptions on the form of the potential when deriving that the slope is to be smaller than $\tan(3\pi/8)$, so that this result is valid irrespective of the potential being used.

We were also able to show some interesting connections concerning the wiggles. First of all, the positions of the spikes seem to be a function of mass-thickness only within a potential family. Changing the depth (and therefore the "attractivity" of the potential) or lowering one of the barriers (in a double barrier case) only shifted the spikes parallel to the real axis. Eventually, when the imaginary part of the localization threshold got smaller than a critical value a new spike was added, but the rest remained qualitatively constant.

The frequency of the wiggles seems to be correlated solely—again within a family of potentials—with the barrier height in such a way that the higher the barrier the smaller the frequency. The thickness-mass does alter the position of the spikes, but not the frequency. The position of the maxima seems to play only a minor role. We also studied the transition from wiggly to nonwiggly behavior by using a potential that includes the above mentioned cases as extreme ones. We found a very smooth transition (see Fig. 12) and no indication of a breakdown of some sort for certain sets of parameters. This might indicate that the possible "mechanism" for the wiggles is not turned on in a sudden fashion, but is rather a continuous process.

As we demonstrated, on the semiclassical level all of the above can be understood by considering the mentioned $\mathrm{Im}\,\alpha_{ij} = 0$ lines and their dependency on, e.g., mass-thickness, etc. One is tempted, really, to say that in the semiclassical description everything is very clear. The difficulty one has, though, is the question of the relevance of concepts like transition points (on which everything depends rather heavily) in the full quantum mechanical picture. Nevertheless, apparently the predictive power of the first order approximation to the full quantum problem is large enough to account for all of the "effects" and to give even a good approximation to the exact values of the spectrum.

One of the goals of this contribution is to stimulate the discussion among mathematicians or mathematical physicists about a general theory dealing with pole string curves of the eigenvalues of complex scaled Hamiltonians. We are well aware of the phenomenological character of our numerical studies and the specific (limited) character of the one-dimensional potential functions used, but on the other hand quite certain that at least some of the facts that we showed here may be proven rigorously. As we demonstrated, the most promising approach is the (multi-turning-point) WKB analysis, not because of the numerical feasibility—which in our eyes is rather limited, especially since one does not know *a priori* how many transition points to use and what order of approximation is sensible—but because of the comparatively simple analytic structure of the (generalized) Bohr-Sommerfeld formula. Further work along these lines is in progress.

ACKNOWLEDGMENTS

It is a pleasure to thank both Erkki Brändas (Uppsala) and Nils Andersson (Cardiff) for many insightful discussions. C.A.C.-D. wishes to thank the members of the faculty of mathematics and natural sciences, Uppsala University, for support. This work was also supported in part by the Fonds der Chemischen Industrie (Frankfurt am Main).

APPENDIX A: POTENTIAL PARAMETERS

Generally, for symmetric potentials, V_u designates the potential minimum, V_0 the potential maximum, and V_t the total height, i.e., $V_t = V_0 - V_u$. The basis set size and integration range were chosen such that we found all resonances to be independent of θ within at least three digits. Atomic units are used throughout.

1. The symmetric double well

$$V(x) = a\left(\tfrac{1}{2}x^2 - b\right)e^{-cx^2}. \tag{A1}$$

This potential has extrema at

$$x_1 = 0, \qquad x_{2/3} = \pm\sqrt{1+2bc} \quad (2cb+1>0), \tag{A2}$$

with

TABLE II. Potential parameters used in the calculations of Fig. 14. Basis set size was 901 and mass 0.7.

a	b	V_u	V_0	V_t
70.00000	0.08	-5.60	10.97	16.57
57.89029	0.15	-8.68	7.89	16.57
45.83412	0.25	-11.46	5.11	16.57
41.33206	0.30	-12.40	4.17	16.57
29.19317	0.50	-14.60	1.98	16.57
16.16950	1.00	-16.17	0.40	16.57
10.98097	1.50	-16.47	0.10	16.57
8.27207	2.00	-16.54	0.03	16.57

$$V_u \equiv V(x_1) = -ba, \qquad V_0 \equiv V(x_{2/3}) = \frac{a}{2}\, e^{-(1+2cb)},$$
$$V_t = V_0 - V_u. \tag{A3}$$

a. Constant total height and c = 1

Table II shows the potential parameters for potentials of type (A1) with constant total height. The fraction of the potential above and below the threshold is varied. Mass thickness is constant.

b. Constant height and c = 1

Table III shows the potential parameters for potentials of type (A1) with constant height above threshold. The depth of the potential is varied, while mass-thickness is kept constant.

c. Constant total height and position of maximum

Table IV shows the potential parameters for potentials of type (A1) with constant total height above thresh-

TABLE III. Potential parameters used in the calculations of Fig. 16. Basis set size was 901 and $\mu = 0.7$.

a	b	V_u	V_0	V_t
10.97000	-1.00	10.97	10.97	0.00
18.50000	-0.60	11.10	11.10	0.00
21.94403	-0.50	10.97	10.97	0.00
26.80250	-0.40	10.72	10.97	0.25
32.73665	-0.30	9.82	10.97	1.15
39.98463	-0.20	8.00	10.97	2.97
44.18986	-0.15	6.63	10.97	4.34
46.92240	-0.12	5.63	10.97	5.34
50.83043	-0.08	4.07	10.97	6.90
59.65007	0.00	0.00	10.97	10.97
65.92352	0.05	-3.30	10.97	14.27
70.00000	0.08	-5.60	10.97	16.57
83.90522	0.17	-14.25	10.97	25.22
98.34633	0.25	-24.59	10.97	35.56
108.68951	0.30	-32.61	10.97	43.58
146.71549	0.45	-66.02	10.97	76.99

TABLE IV. Potential parameters used in the calculations of Fig. 17. Basis set size was 901 and $\mu = 0.7$.

a	b	c	V_u	V_0	V_t
310.98426	0.30	1.78571	-93.30	10.97	104.27
132.85361	0.20	1.31579	-26.57	10.97	37.54
70.00000	0.08	1.00000	-5.60	10.97	16.57
51.42247	0.00	0.86207	0.00	10.97	10.97
29.58890	-0.20	0.64103	5.92	10.97	5.05
10.02430	-1.00	0.31646	10.02	10.97	0.95

TABLE V. Potential parameters used in the calculations of Fig. 13. Basis set size was 901 and $\mu = 0.7$.

a	b	c	V_u	V_0	V_t
70.00000	0.08	1.00000	-5.60	10.97	16.57
32.94118	0.17	1.21951	-5.60	3.28	8.88
28.00000	0.20	1.31579	-5.60	2.31	7.91
11.20000	0.50	6.25000	-5.60	0.00	5.60

TABLE VI. Potential parameters used in the calculations of Fig. 15. $V_{\rm I}$ refers to the left barrier height, while $V_{\rm II}$ refers to the right one. Basis set size was 901 and $\mu = 0.7$

a	b	$V_{\rm I}$	$V_{\rm II}$	V_u
7.5	0.0	11.04	11.04	0.00
7.0	0.3	9.54	11.08	-0.04
6.7	0.5	8.65	11.11	-0.10
6.4	0.7	7.81	11.10	-0.19
6.0	1.0	6.70	11.10	-0.37

TABLE VII. Potential parameters used in the calculations of Fig. 8. $V_{\rm I}$ refers to the left barrier height and $V_{\rm II}$ to the right one. Note that for $a < 3.095$ there is only one barrier. Basis set size was 701 and $\mu = 1$.

a	b	$V_{\rm I}$	$V_{\rm II}$	V_u
6.600	0.0	10.89	10.89	0.00
6.000	1.0	7.29	10.75	-0.04
5.500	2.0	4.34	10.97	-0.18
4.900	3.0	1.56	10.91	-0.47
3.095	6.0		10.97	
0.400	10.0		10.94	

TABLE VIII. Potential parameters as used in Fig. 12. Basis set size was 701 and $\mu = 0.7$.

a	b	V_u	V_0
0.10	1.00	-5.60	9.86
0.30	1.00	-5.60	8.02
0.60	1.00	-5.60	5.96
1.00	1.00	-5.60	4.11

old. In addition to varying the fraction of the potential above or below the threshold, mass-thickness is also varied in order to get constant position of the barrier maxima ($\pm\sqrt{1+2bc}$ is constant).

d. Constant depth and position of maximum

Table V shows the potential parameters for potentials of type (A1) with constant depth. In addition to varying the height of the potential barriers, mass-thickness is also varied in order to get constant position of the barrier maxima ($\pm\sqrt{1+2bc}$ is constant).

2. The asymmetric double well

$$V(x) = a\left(4x^2 - bx\right)e^{-x^2} \tag{A4}$$

(see Table VI). Depending on the choice of the constant b this potential features two barriers of unequal height. We kept one of them constant and varied the height of the other. Mass thickness was constant.

3. The asymmetric x^4 potential family

$$V(x) = -x^4 + ax^2 + bx \tag{A5}$$

(see Table VII). Depending on the choice of the constant b this potential features two barriers of unequal height. We kept one of them constant and varied the height of the other. Mass-thickness was constant. Note that this potential is not dilatation analytic, because it drops to $-\infty$ for $|x| \to \pm\infty$; see, however, Sec. IV.

4. The transition from wiggly to smooth

$$V(x) = 70\left(\tfrac{1}{2}x^2 - 0.08\right)e^{-ax-bx^2} \tag{A6}$$

(see Table VIII). This potential includes as extreme cases ($a = 0$ or $b = 0$) potentials which definitely show wiggles or not, respectively. It is used to study the transition between these two different types of spectra.

5. First order polynomial times Gaussian damping factor

$$V(x) = a\,(x+b)\,e^{-x^2} \tag{A7}$$

(see Table IX). This potential family features one well and one barrier. The barrier height was kept (roughly) constant and the depth of the well was varied in order to study the composite type of resonance spectra. Mass-thickness was kept constant.

TABLE IX. Potential parameters as used in Fig. 6. Basis set size was 901 and $\mu = 5$.

a	b	V_u	V_0
25.00	0.00	-10.72	10.72
13.50	0.50	-2.48	10.51
8.97	1.00	-0.51	10.72
5.10	2.00	-0.01	10.79

6. Piecewise defined potential with two thresholds

$$V(x) = \begin{cases} 70\left(\frac{1}{2}x^2 - 0.08\right)e^{-x^2}, & x \le 0, \\ 70\left(\frac{1}{2}x^2 - 0.294286\right)e^{-x^2} + 15.0, & x > 0. \end{cases} \tag{A8}$$

This potential has two thresholds: one at 0 and one at 15 hartree. The mass was chosen to be 5 and basis set size was 701. See Fig. 10 and the text for details.

APPENDIX B: COMPLEX SCALING

We do not wish to give a complete introduction to complex scaling here; that has been done elsewhere [6,7,45]. The purpose of this section is to define our nomenclature and to remind the reader of the important theorems in this context.

One could summarize the purpose of complex scaling for this kind of application as the following. While standard time-independent quantum mechanics is clearly relevant for all bound state problems, it cannot deal with quasibound particles, i.e., with resonant behavior, consistently. This has been known at least since the Gamow theory of α decay [22].

Therefore an extension to the theory has been developed [1–3]. The main tool has been to transform the Schrödinger equation by a nonunitary transformation, which is (for uniform scaling) defined by

$$U(\theta) = \exp\left(-\frac{\theta}{2}(xp+px)\right), \quad \theta \in \mathbb{R}, \tag{B1}$$

which leads to

$$Uf(x) = \eta^{1/2} f(\eta x), \eta = e^{i\theta}, \tag{B2}$$

$$H(\eta) = U(\eta) H U^{-1}(\eta). \tag{B3}$$

The eigenvalues of the transformed Hamiltonian $H(\eta)$ are complex numbers. The imaginary part is interpreted as being proportional to the inverse of the lifetime. Via the transformation the eigenvalues of the kinetic energy operator, which constitute the branch cut of the resolvent, are rotated into the fourth quadrant of the complex energy plane by -2θ, thereby opening the second unphysical sheet. Eigenvalues on that sheet are called resonances. (One should mention here, though, that there are indeed different ways to define a resonance; see, e.g., [46].) Those eigenvalues do not depend on the parameter θ,

$$\frac{\partial E}{\partial \eta} \propto \frac{\partial E}{\partial \theta} = 0, \tag{B4}$$

i.e., they fulfill a stationarity principle [47,48] and—as is known—a complex virial theorem [47].

When using complex scaling one has to use a "new" scalar product (which, naturally, reduces to the standard $\mathcal{L}^2$ scalar product for $\theta = 0$)

$$\langle \psi \mid \psi \rangle \equiv \int [\psi(\eta^* x)]^* \psi(\eta x) \eta \, dx. \tag{B5}$$

For a discussion of the scalar product see [49] and especially [50]. Let us note that there are numerous ways to distort the path into the complex plane [46,51]. We have used only uniform scaling—as defined by Eq. (B1)—because we found it to be numerically the most stable.

For our numerical studies we employed the complex scaled Fourier grid Hamiltonian method (CSFGH), which was presented by Chu [31], and—when in doubt—direct integration methods like the renormalized Numerov or the log-derivative method [37–39]. The CSFGH method is a very fast and very accurate method. Under our "extreme" conditions (the angles θ were rather large, namely, between 0.7 and 0.775 rad; for the simple Gaussian type potentials in Fig. 4 even up to 0.782 rad) the lowest resonances were constant under variation of θ up to eight digits (direct integration methods perform better here). We required for the higher resonances at least three significant digits. Basis set size was generally 701–901 and the mass was varied—depending naturally on the potential—between 0.4 and 20 a.u.

[1] J. Nuttall and H. Cohen, Phys. Rev. **188**, 1542 (1969).
[2] J. Aguilar and J. Combes, Commun. Math. Phys. **22**, 269 (1971).
[3] E. Balslev and J. Combes, Commun. Math. Phys. **22**, 280 (1971).
[4] B. Simon, Ann. Math. **97**, 247 (1973).
[5] *Resonances: The Unifying Route towards the Formulation of Dynamical Processes,* edited by E. Brändas and N. Elander, Lecture Notes in Physics Vol. 325 (Springer-Verlag, Berlin, 1989).
[6] Int. J. Quantum Chem. **14**, No. 4 (1978).
[7] Int. J. Quantum Chem. **31**, No. 5 (1987).
[8] C.A. Chatzidimitriou-Dreismann, Adv. Chem. Phys. **80**, 201 (1991).
[9] V.I. Kukulin, V.M. Krasnopol'sky, and J. Horáček, *Theory of Resonances: Principles and Applications* (Kluwer Academic Publishers, Dordrecht, 1989).
[10] R.G. Newton, *Scattering Theory of Waves and Particles,* 2nd ed. (Springer-Verlag, Berlin, 1982).
[11] A. Böhm, J. Math. Phys. **22**, 2813 (1981).
[12] M. Rittby, N. Elander, and E. Brändas, Phys. Rev. A **24**, 1636 (1981).
[13] M. Rittby, N. Elander, and E. Brändas, Mol. Phys. **45**, 553 (1982).
[14] M. Rittby, N. Elander, and E. Brändas, Phys. Rev. A **26**, 1804 (1982).
[15] H. Korsch, in *Resonances—Models and Phenomena,* edited by S. Albeverio, L. S. Ferreira, and L. Streit, Lecture Notes in Physics Vol. 211 (Springer-Verlag, Berlin, 1984), pp. 217–234.
[16] J. Connor, Mol. Phys. **25**, 1469 (1973).
[17] N. Fröman and P. Fröman, in *Forty More Years of Ramifications: Spectral Asymptotics and its Applications,* edited by S. A. Fulling and F. J. Narcowich, Discourses in Mathematics and its Applications, Vol. 1 (Texas A&M University, College Station, 1992), pp. 121–159.
[18] P. Löwdin, P. Froelich, and M. Mishra, Adv. Quantum Chem. **20**, 185 (1989).
[19] G. Doolen, J. Nuttall, and R.W. Stagat, Phys. Rev. A **10**, 1612 (1974).
[20] Y.K. Ho, Phys. Rep. C **99**, 1 (1983).
[21] N. Moiseyev, N. Lipkin, D. Farrelly, O. Atabek, and R. Lefebvre, J. Chem. Phys. **91**, 6246 (1989).
[22] G. Gamow, Z. Phys. **51**, 204 (1928).
[23] M. Child, J. Mol. Spectrosc. **53**, 280 (1974).
[24] T. Seideman and W. Miller, J. Chem. Phys. **95**, 1768 (1991).
[25] B. Böhmer, H. Lehr, and C.A. Chatzidimitriou-Dreismann (unpublished).
[26] J. Korsch, H. Laurent, and R. Möhlenkamp, Phys. Rev. A **26**, 1802 (1982).
[27] N. Andersson, Int. J. Quantum Chem. **46**, 375 (1993).
[28] A.F.J. Siegert, Phys. Rev. **57**, 750 (1939).
[29] J.R. Taylor, *Scattering Theory* (Wiley, New York, 1972).
[30] R. Yaris, J. Bendler, R.A. Lovett, C.M. Bender, and P. Fedders, Phys. Rev. A **18**, 1816 (1978).
[31] S.-I. Chu, Chem. Phys. Lett. **167**, 155 (1990).
[32] H. Lehr and C.A. Chatzidimitriou-Dreismann, Chem. Phys. Lett. **201**, 278 (1993).
[33] H. Lehr and C.A. Chatzidimitriou-Dreismann, Chem. Phys. Lett. **186**, 511 (1991).
[34] H. Lehr, C.A. Chatzidimitriou-Dreismann, and E. Brändas, Phys. Scr. **49**, 528 (1994).
[35] H. Korsch, H. Laurent, and R. Möhlenkamp, J. Phys. B **15**, 1 (1982).
[36] E. Brändas, M. Rittby, and N. Elander, J. Math. Phys. **26**, 2648 (1985).
[37] B. Johnson, J. Comput. Phys. **13**, 445 (1973).
[38] B. Johnson, J. Chem. Phys. **67**, 4086 (1977).
[39] B. Johnson, J. Chem. Phys. **69**, 4678 (1978).
[40] J. Caballero Carretero and A. Martin Sánchez, J. Math. Phys. **28**, 636 (1987).
[41] *Handbook of Mathematical Functions,* edited by M. Abramowitz and I. Stegun (Dover, New York, 1972).
[42] N. Moiseyev, P.R. Certain, and F. Weinhold, Int. J. Quantum Chem. **14**, 727 (1978).
[43] R. Bain, J.N. Bardsley, B.R. Junker, and C. Sukumar, J. Phys. B **7**, 2189 (1974).
[44] N. Andersson (unpublished).
[45] P. Löwdin, Adv. Quantum Chem. **19**, 87 (1988).
[46] B. Simon, Int. J. Quantum Chem. **14**, 529 (1978).
[47] E. Brändas and P. Froelich, Phys. Rev. A **16**, 2207 (1977).
[48] D. Truhlar and C. Mead, Phys. Rev. A **42**, 2593 (1990).
[49] N. Elander and E. Brändas, in *Resonances: The Unifying Route towards the Formulation of Dynamical Processes,* edited by E. Brändas and N. Elander, Lecture Notes in Physics Vol. 325 (Springer-Verlag, Berlin, 1989), pp. 541–552.
[50] A. Scrinzi and N. Elander, J. Chem. Phys. **98**, 3866 (1993).
[51] I. Sigal, Ann. Inst. Henri Poincaré **41**, 103 (1984).